NANO LETTERS

Letter

pubs.acs.org/NanoLett

Nano-FTIR Absorption Spectroscopy of Molecular Fingerprints at 20 nm Spatial Resolution

Florian Huth,[†,‡] Alexander Govyadinov,[†] Sergiu Amarie,[§] Wiwat Nuansing,[†] Fritz Keilmann,[∥] and Rainer Hillenbrand*[,†,⊥]

[†]CIC nanoGUNE Consolider, 20018 Donostia - San Sebastián, Spain

[‡]Neaspec GmbH, 82152 Martinsried, Germany

[§]Max Planck Institute of Quantum Optics, 85714 Garching, Germany

[∥]Department of Physics and CeNS, Ludwigs-Maximilians-Universität München, 85714 Garching, Germany

[⊥]IKERBASQUE, Basque Foundation for Science, 48011 Bilbao, Spain

Supporting Information

ABSTRACT: We demonstrate Fourier transform infrared nanospectroscopy (nano-FTIR) based on a scattering-type scanning near-field optical microscope (s-SNOM) equipped with a coherent-continuum infrared light source. We show that the method can straightforwardly determine the infrared absorption spectrum of organic samples with a spatial resolution of 20 nm, corresponding to a probed volume as small as 10 zeptoliter (10^{-20} L). Corroborated by theory, the nano-FTIR absorption spectra correlate well with conventional FTIR absorption spectra, as experimentally demonstrated with poly-(methyl methacrylate) (PMMA) samples. Nano-FTIR can thus make use of standard infrared databases of molecular vibrations to identify organic materials in ultrasmall quantities and at ultrahigh spatial resolution. As an application example we demonstrate the identification of a nanoscale PDMS contamination on a PMMA sample.

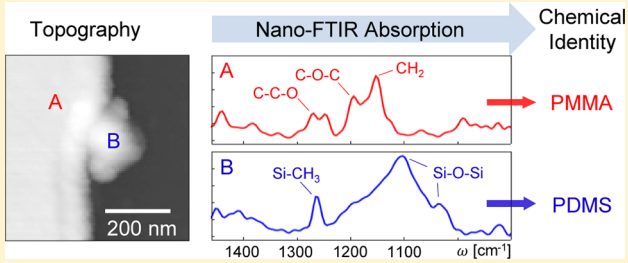

KEYWORDS: *Infrared nanospectroscopy, chemical identification, polymers, near-field microscopy, s-SNOM, FTIR*

The chemical composition of molecular thin films and nanocomposites plays a key role in the development of nanoscale devices or biocompatible surfaces. A widely used tool for chemical recognition is Fourier transform infrared (FTIR) spectroscopy[1] which determines fingerprint absorption spectra in the 400−4000 cm^{-1} mid-infrared frequency region (corresponding to wavelengths of 2.5−25 μm). A comparison of these spectra with widely established databases enables a rapid identification of materials and thus is commonly used in analytical chemistry, biology, and even medicine.[1] The spatial resolution of FTIR microscopy, however, is limited by diffraction to about one wavelength and thus does not allow for resolving features smaller than a few micrometers.

Ultraresolving infrared microscopy has recently become possible with the introduction of scattering-type scanning near-field optical microscopy (s-SNOM),[2] which can be regarded as an extended atomic force microscopy (AFM) that returns an infrared image together with topography. As sketched in Figure 1a, an illuminating infrared beam is focused onto the probing tip. The usually chosen metallic tip acts as an antenna, concentrating the incident light at the apex of the tip. The scattering from the tip depends on the near-field interaction between the tip and the sample. Recording the scattered light, while scanning the sample surface, thus yields a near-field image. Its resolution is not dependent on the illumination wavelength, but only on the size of the tip apex, which is typically in the order of 20 nm.[2]

Using s-SNOM, nanoscale infrared imaging and spectroscopy of molecular vibrations in the 6 μm wavelength region have been successfully demonstrated with polymer and protein nanostructures,[3−6] including single viruses[7] and fibrils.[8] In these experiments, the illumination of the tip was provided by tunable CO gas lasers. However, such lasers offer only a relatively narrow spectral bandwidth, and local spectroscopy requires repeated imaging at different wavelengths. These disadvantages have triggered the development and application of broadband infrared sources for s-SNOMs. Recently, several solutions were presented that enable the realization of broadband infrared nanospectroscopy,[9−12] among them (i) the use of a thermal incoherent infrared emitter,[9] and (ii) the use of a laser-based coherent infrared continuum source[13,14] for illuminating the s-SNOM tip (nano-FTIR). However, due to the limited power of these sources, only strong phonon and plasmon resonances could be mapped, but not the vibrational contrasts of molecular organic substances which rely on relatively weak resonances.[15]

Received: March 26, 2012
Revised: June 1, 2012
Published: June 15, 2012

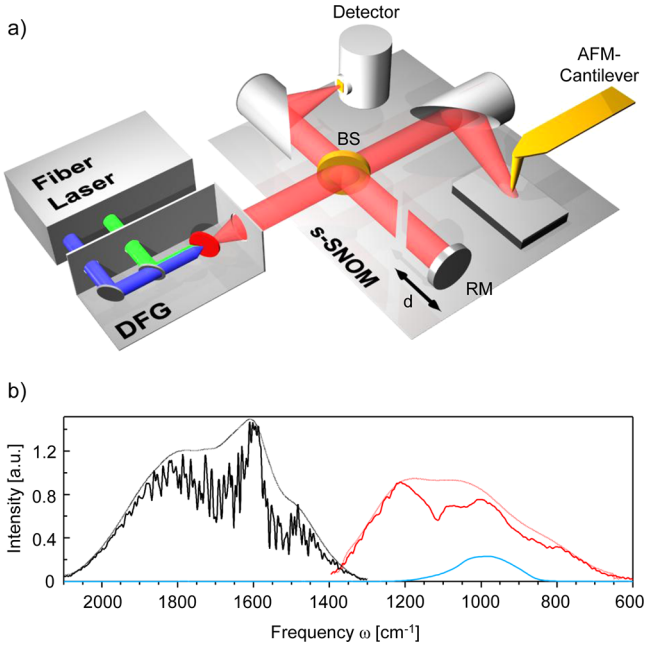

Figure 1. Nano-FTIR operated with a coherent mid-infrared continuum source. (a) Experimental setup, showing the Er-fiber-laser system that emits a pulse train at 1.55 μm (blue) and another one which is broadened and red-shifted (green). A difference frequency generator (DFG) unit superimposes both beams in a nonlinear crystal, which subsequentially emits a mid-infrared (MIR) continuum beam that is used for illuminating the AFM tip of the nano-FTIR. The backscattered light is analyzed with an asymmetric Michelson interferometer comprising a beamsplitter (BS) and a reference mirror (RM). (b) Output spectra for two settings of the MIR continuum covering either the lower-frequency fingerprint region 700−1400 cm^{-1} (red) or the higher-frequency fingerprint region 1300−2100 cm^{-1} (black). Measurements were taken approximately 2 m away from the source. The fine curves represent the source spectra corrected for atmospheric absorption. For comparison, the blue line shows the output spectrum of a previous DFG implementation.[16]

Here we demonstrate for the first time that nano-FTIR can acquire molecular vibrational spectra throughout the mid-infrared fingerprint region at a spatial resolution of 20 nm, by imaging a typical polymer sample (poly(methyl methacrylate), PMMA). This became possible by combining the nano-FTIR setup with a novel laser-based infrared continuum source, which is able to provide broadband illumination of sufficient power for detecting the weak molecular vibrational resonances of organic samples. We furthermore provide first experimental evidence that the near-field absorption spectra match well with conventional (far-field) FTIR absorption spectra and corroborate this observation theoretically. This relates, in particular, to the spectral line positions, line widths and line shapes, and therefore allows for direct chemical recognition of nanoscale materials by consulting standard FTIR databases.

For our experiments we use a commercial s-SNOM (NeaSNOM, neaspec.com) comprising an AFM and an asymmetric Michelson interferometer (Figure 1a). A standard Au-coated AFM-tip is illuminated by a coherent broadband mid-infrared beam. The beam is generated by a difference frequency generator (DFG, lasnix.com), where two near-infrared, 100-fs pulse trains from a fiber-laser system (FemtoFiber pro IR and SCIR, toptica.com) are superimposed in a GaSe crystal. Compared to an earlier implementation,[16] the mid-infrared output power is substantially increased to 0.25 mW. This mid-infrared source emits a continuous spectrum with a usable width up to 700 cm^{-1}, which can be tuned within the limits 700−2500 cm^{-1} dependent on DFG settings (e.g. the crystal orientation). Figure 1b shows two mid-infrared output spectra (red and black) for two selected settings that were used in the presented experiments. Clearly, already these two settings suffice for a nearly complete coverage of the central 700−2100 cm^{-1} (5−14 μm) molecular infrared fingerprint region. For comparison we show the output spectrum of ref 16 (blue line), clearly illustrating the significant enhancement of both spectral coverage and spectral intensity achieved with our new DFG setup.

The light backscattered from the oscillating metallic tip is analyzed with an asymmetric Fourier transform spectrometer,[9,16,17] which is based on a Michelson interferometer. In contrast to conventional FTIR, the sample (together with the tip) is located in one of the interferometer arms (Figure 1a). This detection scheme allows for recording both the amplitude $s(\omega)$ and phase $\varphi(\omega)$ spectra of the backscattered light. The pertaining complex-valued scattering coefficient $\sigma(\omega) = s(\omega)e^{i\varphi(\omega)}$ relates the scattered field $E(\omega)$ with the incident field $E_{inc}(\omega)$ according to $E(\omega) = \sigma(\omega)E_{inc}(\omega)$. To extract the near-field signals, that is, to suppress background contributions, the detector signal is demodulated at a higher harmonic nΩ of the tip vibration frequency Ω (refs 18 and 19). Translation of the reference mirror with a piezo stage yields an interferogram of the demodulated signal. By subsequent Fourier transformation of the interferogram we obtain the complex-valued near-field spectra $E_n(\omega) = \sigma_n(\omega)R(\omega)E_{inc}(\omega)$ where the index n denotes the demodulation order and $R(\omega)$ is the spectral response of the instrument including the transmission of the beamsplitter, atmospheric absorption, and responsivity of the infrared detector. Analogue to conventional FTIR, the near-field spectra $E_n(\omega)$ are normalized with the help of a reference spectrum $E_{n,ref}(\omega)$. The latter can be readily obtained by recording a near-field spectrum of a spectrally flat sample such as Si (where $\sigma_{n,Si}(\omega) = \text{const}$), yielding $E_{n,ref}(\omega) = \text{const}\ R(\omega)E_{inc}(\omega)$. The normalized near-field spectra thus directly yield the n-th order scattering coefficient of the tip−sample system, $\sigma_n(\omega) \propto E_n(\omega)/E_{n,ref}(\omega)$.

The scattering coefficient $\sigma_n(\omega)$ describes the near-field interaction between tip and sample and carries information about the local dielectric function, respectively, the refractive index, of the sample. Earlier experiments with organic samples indicate that the phase $\sigma_n(\omega)$, respectively the imaginary part $\text{Im}[\sigma_n(\omega)] = s_n(\omega)\sin[\varphi_n(\omega)]$, is connected with the local absorption of the sample.[3,8,20] Owing to the lack of broadband near-field spectra, however, a clear experimental demonstration with molecular fingerprint spectra has not been provided yet, nor has a rigorous physical derivation been put forward. Here we define the nano-FTIR absorption to be $a_n \equiv \text{Im}[\sigma_n(\omega)]$ and verify experimentally and theoretically that nano-FTIR absorption spectra of molecular vibrations correlate well with conventional far-field absorption spectra.

First we demonstrate the capabilities of our setup for nanoscale-resolved infrared imaging by mapping the boundary region of a 90 nm thin film of PMMA on a Si substrate. The s-SNOM simultaneously records a topographical (Figure 2a, upper image) and a near-field infrared image (Figure 2a, lower image). For the latter we fix the reference arm of the Michelson interferometer at approximately the "white light position" (WLP). In this case both interferometer arms have equal optical path lengths. Thus all frequencies are in phase, creating

dx.doi.org/10.1021/nl301159v | Nano Lett. 2012, 12, 3973−3978

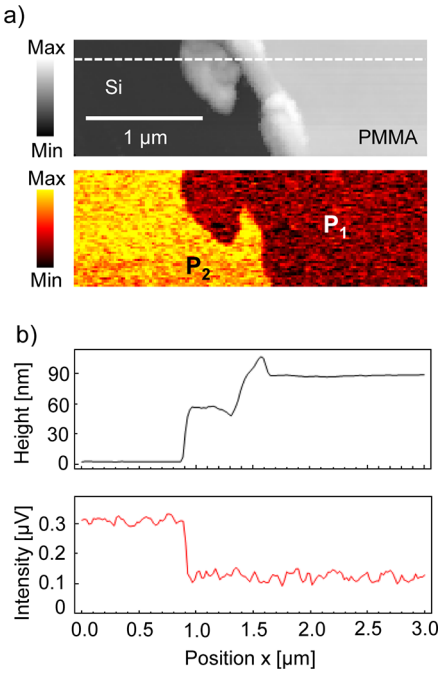

Figure 2. Infrared nanoimaging of a polymer thin film (PMMA) on a Si substrate. (a) Topography (upper) and infrared amplitude image (lower, spectrally averaged over approximately 5−9 μm by setting the interferometer at the WLP). (b) Line profiles of height and infrared signal extracted at the position indicated by the white dashed line (averaged over eight lines).

a maximum detector signal. In the optical image we observe a strong material contrast between the PMMA and the Si regions. The stronger infrared signal on Si can be explained by its higher refractive index compared to PMMA.[21] The abrupt signal change at the material boundary verifies the nanoscale spatial resolution. We note that the infrared signal on the PMMA does not depend on the different heights of the PMMA surface in the edge region of the film. This indicates that the probing depth of the near-field interaction[22,23] is smaller than the thickness of the PMMA film.

To demonstrate local fingerprint spectroscopy, we recorded nano-FTIR spectra of PMMA and Si at the positions marked with P_1 and P_2 in Figure 2a. Owing to the flat spectral response of Si, the spectrum at P_2 serves as reference spectrum (as described above), yielding the local absorption spectrum of PMMA, $a_2(\omega) \propto P_1/P_2$. The broadband mid-infrared source was first set to cover the frequency range 1300−2100 cm^{-1}. For a second set of spectra the source was set to the frequency range 700−1400 cm^{-1}. The resulting nano-FTIR absorption spectra $a_2(\omega)$ are displayed in Figure 3a. For comparison, a FTIR absorption spectrum (Figure 3b) of a PMMA film (thickness of ∼5 μm, produced by a solvent-casting method) was recorded with a conventional FTIR spectrometer (Equinox 55, bruker.com) in transmission mode. The FTIR spectrum shows the well-known molecular absorption lines of PMMA[24,25] around 1730 cm^{-1} (corresponding to C═O stretching), 1265 cm^{-1} and 1240 cm^{-1} (C−C−O stretching), 1190 cm^{-1} (C−O−C bending), and 1145 cm^{-1} (CH_2 bending). Convincingly, all of these lines are also clearly seen in the nano-FTIR absorption spectrum. As documented by the dashed gray lines in Figure 3, the near-field absorption peaks appear at the same positions as the far-field absorption peaks. The overall agreement of peak positions, peak shapes and relative peak heights provides clear experimental evidence that the nano-FTIR absorption $a_n = \mathrm{Im}[\sigma_n(\omega)]$ indeed reveals the local infrared absorption of the sample.

The direct correlation between conventional and nano-FTIR absorption spectra might be surprising when considering that nano-FTIR records the scattered light arising from a complex near-field interaction between tip and sample. We explain this

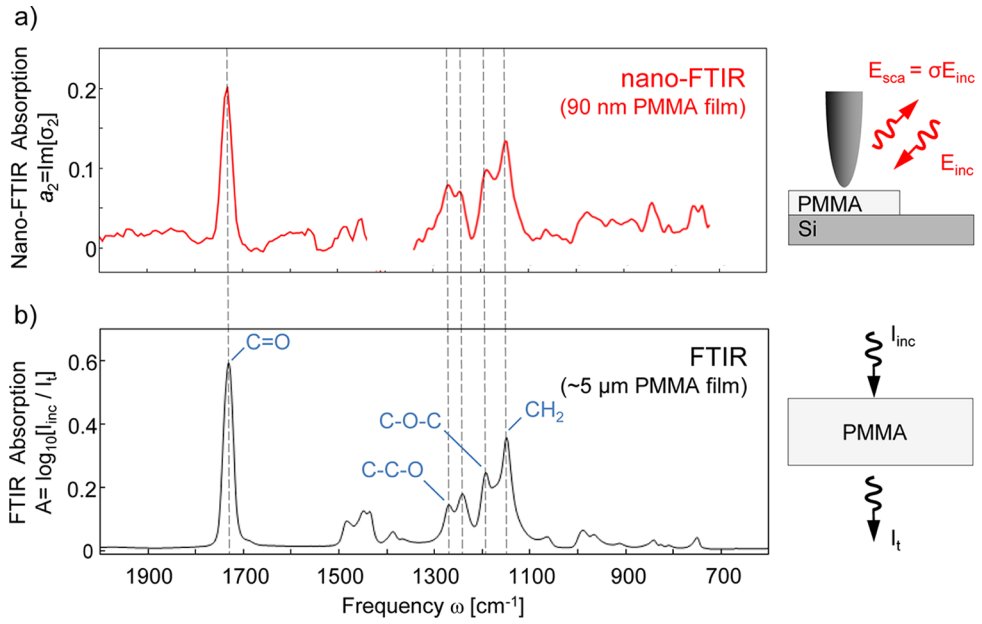

Figure 3. Comparison of nano-FTIR with conventional far-field FTIR. (a) Nano-FTIR absorption spectra from a 90 nm thin film of PMMA. (b) Far-field FTIR spectra from a ∼5 μm thick PMMA film. The nano-FTIR data is obtained from two consecutive measurements where the infrared source spectrum was changed from (2000 to 1400 cm^{-1}) to (1400 to 800 cm^{-1}). The acquisition time was 25 min and 16 min, respectively, and the spectral resolution is 6 cm^{-1}. The far-field FTIR spectrum was taken in 20 min with a spectral resolution of 4 cm^{-1}. The schematics to the right of the spectra illustrate nano-FTIR and standard transmission FTIR.

dx.doi.org/10.1021/nl301159v | Nano Lett. 2012, 12, 3973−3978

intriguing phenomenon by theoretical considerations of the scattering process. It has been shown formerly that the scattering coefficient σ can be successfully described by the point-dipole model[2] and more accurately by the finite-dipole model.[26] In both models, the scattering coefficient σ has the same structure:

$$\sigma(\omega, H) = \alpha_{\mathrm{eff}}(f\beta)(1 + r_s)^2 \quad (1)$$

where α_{eff} $(f\beta)$ is the effective polarizability of the tip and r_s the far-field reflection coefficient of the sample surface. $\beta = \beta(\omega) = (\varepsilon(\omega) - 1)/(\varepsilon(\omega) + 1)$ is the surface response function, which is dependent on the complex-valued dielectric function $\varepsilon(\omega)$ of the sample. $f = f(H)$ is a (model-specific) frequency-independent function of the tip−sample distance H. For studies of thin films with a thickness $\Delta \ll \lambda$ (for infrared light: $\lambda \sim 10\ \mu m$), r_s can be well-approximated by the Fresnel reflection coefficient from the substrate. In case the substrate is spectrally flat, like the Si in our experiment, the reflection r_s can be considered as spectrally constant. In the absence of infrared plasmon or geometrical antenna resonances[27−29] in the tip, and for a thin film composed of weak molecular oscillators, such as PMMA or other organic materials, the condition $|f\beta| < 1$ is always satisfied. Therefore we can expand $\sigma(\omega, H)$ into a Taylor series, which to the first order in $(f\beta)$ yields:

$$\sigma(\omega, H) \approx [\alpha_0 + \alpha_1 f(H)\beta(\omega)](1 + r_s)^2 \quad (2)$$

where α_0 and α_1 are frequency- and height-independent constants that are determined by the material and the size of the tip. Taking into account the demodulation of the detector signal, which is applied for background suppression in our experiments, and the normalization of the sample spectra to those of Si, all height-independent terms vanish, yielding

$$\sigma_n(\omega) \propto \beta(\omega) \quad (3)$$

Thus, the spectral characteristics of the near-field absorption $a_n = \mathrm{Im}[\sigma_n(\omega)] \propto \mathrm{Im}[\beta(\omega)]$ are determined exclusively by the local dielectric function $\varepsilon(\omega)$ of the sample. For molecular vibrations, such as the ones of PMMA, we find that $\mathrm{Im}[\beta(\omega)]$ and the imaginary part κ of the complex-valued refractive index $N(\omega) = n(\omega) + i\kappa(\omega)$ have nearly the same spectral behavior (see supplement), and we can write in good first approximation $\kappa(\omega) \sim \mathrm{Im}[\beta(\omega)]$. Considering that the far-field absorption A in conventional FTIR spectroscopy follows the relation $A \propto \kappa(\omega)$, we immediately obtain $a_n(\omega) \propto \mathrm{Im}[\beta(\omega)] \propto \kappa(\omega) \propto A$. The connection between near-field and far-field absorption is thus described in good approximation by the simple and model-independent relation

$$a_n(\omega) \propto A \quad (4)$$

which theoretically explains the experimental observation documented in Figure 3 and provides a firm ground for chemical recognition and possibly even chemometrics at nanoscale spatial resolution.

In Figure 4 we demonstrate nanoscale spectroscopic mapping of the local infrared absorption. While scanning the tip across the PMMA edge (Figure 4a), an infrared spectrum is recorded at each position. Each panel of Figure 4b shows 50 spectra, every single one recorded in 80 s and with 13 cm^{-1} spectral resolution. The distance between the points at which the spectra are acquired is 20 nm. As before all spectra are normalized to the reference spectrum taken on the Si surface. On the PMMA we clearly see the characteristic absorption

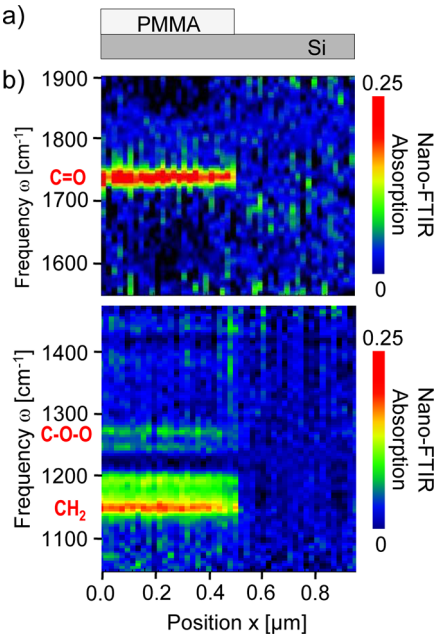

Figure 4. Nanoscale infrared-spectroscopic mapping of PMMA on Si. (a) Schematics of the sample cross section. (b) Infrared-spectroscopic line scans recorded while the tip was scanned in 20 nm steps (horizontal axis) across the sample illustrated in Figure 4a. Each panel is composed of 50 spectra (vertical axis) acquired with the coherent source set to cover the 1000−1500 cm^{-1} (bottom) and 1500−1900 cm^{-1} (top) spectral ranges.

lines. The peak maxima are nearly constant until the edge is reached at $x = 0.5\ \mu m$. Within a single scan step, the strong C═O and CH_2 absorption peaks vanish completely. This observation confirms that infrared fingerprint spectroscopy can be performed at 20 nm spatial resolution. Because the probing depth of the near-field interaction approximately equals the lateral spatial resolution,[22,23,30] we further conclude that the probed volume is as small as $(20\ nm)^3 = 10^{-20}$ L = 10 zL (10 zeptoliter). We note that the spatial resolution in s-SNOM is determined essentially by the radius of the tip apex,[2] which is about 20 nm in our experiments. Decreasing the scan step below 20 nm thus would not improve the spatial resolution.

Finally we demonstrate the identification of sample contaminants as an application example of nano-FTIR. Figure 5a shows the topography image of a scratched PMMA film on a Si substrate, revealing a particle-like feature at the PMMA edge, which in the mechanical AFM phase image (Figure 5b) exhibits a strong phase contrast of about 70°. Such phase contrasts indicate different materials.[31] Without prior knowledge, however, we cannot identify the particle-like feature of about 100 nm diameter. By taking a nano-FTIR absorption spectrum (lower panel in Figure 5c) in the center of the particle (marked with P_4), we find a significantly different spectral signature compared to the spectrum taken on the PMMA film at the position marked with P_3. While the latter exhibits the known PMMA vibrational fingerprint (as seen before in Figures 3 and 4), we find at P_4 a strong and broad peak centered around 1100 cm^{-1}, a sharper peak around 1260 cm^{-1}, and a small peak around 1040 cm^{-1}. With the help of conventional FTIR spectra from literature, we can assign the peak around 1260 cm^{-1} to the Si-CH_3 symmetric deformation and the broad peak around 1100 cm^{-1} as well as the peak around 1040 cm^{-1} to Si−O−Si asymmetric stretching modes.[32] The appearance of these

dx.doi.org/10.1021/nl301159v | Nano Lett. 2012, 12, 3973−3978

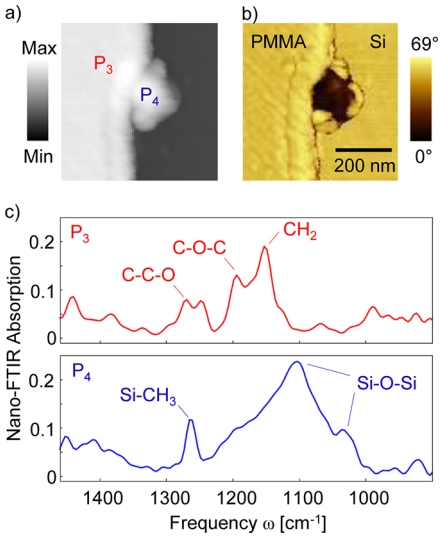

Figure 5. Chemical identification of nanoscale sample contaminations with nano-FTIR. (a) AFM topography image of a scratched PMMA film on a Si substrate. (b) Mechanical AFM phase image, where the strong contrast designates a particle that consists neither of PMMA nor of Si. (c) Nano-FTIR absorption spectra of the PMMA film (taken at position P_3) and of the particle (taken at position P_4). The acquisition time was 7 min, and the spectral resolution is 13 cm^{-1}.

spectral lines is typical for polydimethylsiloxane (PDMS).[32] We can thus identify the particle-like feature as a PDMS contamination. We note that the PMMA sample preparation and precharacterization involved PDMS material, obviously leaving PDMS remainders on the sample surface.

In conclusion, nano-FTIR with a coherent mid-infrared continuum source enables a full spectroscopic analysis of molecular vibrations on the nanometer scale in the important mid-IR frequency range 800−2000 cm^{-1}. We have shown experimentally and theoretically that nano-FTIR absorption spectra correlate well with conventional (far-field) FTIR absorption spectra. Nano-FTIR thus opens the door to nanoscale chemical identification of virtually any substance exhibiting IR vibrational resonances, in ultrasmall quantities and at ultrahigh spatial resolution, by simply searching for the corresponding spectra in standard FTIR databases. We envision, for example, nanoscale chemical mapping of polymer blends, organic fibers, and biomedical tissue. We furthermore established a simple relation between nano-FTIR spectra and the dielectric response of the sample, which in the future will allow for straightforward reconstruction of both the real and imaginary part of the local refractive index, respectively the local dielectric function $\varepsilon(\omega)$ of organic, molecular, and biological materials, nanocomposites, or nanodevices.

■ ASSOCIATED CONTENT

Supporting Information

Relation between $\mathrm{Im}[\beta(\omega)]$ and $\kappa(\omega)$. This material is available free of charge via the Internet at http://pubs.acs.org.

■ AUTHOR INFORMATION

Corresponding Author

*E-mail: r.hillenbrand@nanogune.eu.

Notes

The authors declare the following competing financial interest(s): F.K. and R.H. are co-founders of Neaspec GmbH, a company producing scattering-type scanning near-field optical microscope systems, such as the one used in this study. All other authors declare no competing financial interests.

■ ACKNOWLEDGMENTS

We thank A. Rebollo for sample preparation and A. Bittner and S. Carney for discussions. This work was financially supported by an ERC Starting Grant No. 258461 (TERATOMO) and the National Project MAT2009-08398 from the Spanish Ministerio de Ciencia e Innovacion and supported by Deutsche Forschungsgemeinschaft through the Cluster of Excellence Munich Centre for Advanced Photonics.

■ REFERENCES

(1) Griffiths, P. R.; de Haseth, J. A. *Fourier Transform Infrared Spectrometry*; Wiley: New York, 2007.
(2) Keilmann, F.; Hillenbrand, R. *Nano-Optics and Near-Field Optical Microscopy*; Artech House: Boston/London, 2008.
(3) Taubner, T.; Hillenbrand, R.; Keilmann, F. Nanoscale polymer recognition by spectral signature in scattering infrared near-field microscopy. *Appl. Phys. Lett.* **2004**, *85*, 5064−5066.
(4) Raschke, M. B.; et al. Apertureless near-field vibrational imaging of block-copolymer nanostructures with ultrahigh spatial resolution. *ChemPhysChem* **2005**, *6*, 2197−2203.
(5) Samson, J.-S.; et al. Characterization of single diamondlike and polymerlike nanoparticles by midinfrared nanospectroscopy. *J. Appl. Phys.* **2009**, *105*, 064908.
(6) Kopf, I.; et al. Chemical Imaging of Microstructured Self-Assembled Monolayers with Nanometer Resolution. *J. Phys. Chem. C* **2007**, *111*, 8166−8171.
(7) Brehm, M.; Taubner, T.; Hillenbrand, R.; Keilmann, F. Infrared spectroscopic mapping of single nanoparticles and viruses at nanoscale resolution. *Nano Lett.* **2006**, *6*, 1307−1310.
(8) Paulite, M.; et al. Imaging Secondary Structure of Individual Amyloid Fibrils of a β2-Microglobulin Fragment Using Near-Field Infrared Spectroscopy. *J. Am. Chem. Soc.* **2011**, *133*, 7376−7383.
(9) Huth, F.; Schnell, M.; Wittborn, J.; Ocelic, N.; Hillenbrand, R. Infrared-spectroscopic nanoimaging with a thermal source. *Nat. Mater.* **2011**, *10*, 352−356.
(10) Amarie, S.; Ganz, T.; Keilmann, F. Mid-infrared near-field spectroscopy. *Opt. Express* **2009**, *17*, 21794−21801.
(11) Jones, A. C.; Raschke, M. B. Thermal infrared near-field optical spectroscopy. *Nano Lett.* **2012**, *12*, 1475−1481.
(12) Lu, F.; Belkin, M. A. Infrared absorption nano-spectroscopy using sample photoexpansion induced by tunable quantum cascade lasers. *Opt. Express* **2011**, *19*, 19942−19947.
(13) Keilmann, F.; Amarie, S. Mid-infrared Frequency Comb Spanning an Octave Based on an Er Fiber Laser and Difference-Frequency Generation. *J. Infrared Milli. Terahz. Waves* **2012**, *33*, 479−484.
(14) Amarie, S.; et al. Nano-FTIR chemical mapping of minerals in biological materials. *Beilstein J. Nanotechnol.* **2012**, *3*, 312−323.
(15) Röseler, A. *Infrared spectroscopic ellipsometry*; Akademie-Verlag: Berlin, 1990.
(16) Amarie, S.; Keilmann, F. Broadband-infrared assessment of phonon resonance in scattering-type near-field microscopy. *Phys. Rev. B* **2011**, *83*, 045404.
(17) Ocelic, N.; Hillenbrand, R. Optical device for measuring modulated signal light. Patent No. EP1770714B1, 2008, and US 7738115 B2, 2010.
(18) Labardi, M.; Patane, S.; Allegrini, M. Artifact-free near-field optical imaging by apertureless microscopy. *Appl. Phys. Lett.* **2000**, *77*, 621−623.
(19) Hillenbrand, R.; Keilmann, F. Complex optical constants on a subwavelength scale. *Phys. Rev. Lett.* **2000**, *85*, 3029−3032.

(20) Stiegler, J. M.; et al. Nanoscale Infrared Absorption Spectroscopy of Individual Nanoparticles Enabled by Scattering-Type Near-Field Microscopy. *ACS Nano* **2011**, *5*, 6494−6499.
(21) Taubner, T.; Hillenbrand, R.; Keilmann, F. Performance of visible and mid-infrared scattering-type near-field optical microscopes. *J. Microscopy* **2003**, *210*, 311−314.
(22) Taubner, T.; Keilmann, F.; Hillenbrand, R. Nanoscale-resolved subsurface imaging by scattering-type near-field optical microscopy. *Optics Express* **2005**, *13*, 8893−8898.
(23) Raschke, M. B.; Lienau, C. Apertureless near-field optical microscopy: Tip-sample coupling in elastic light scattering. *Appl. Phys. Lett.* **2003**, *83*, 5089−5091.
(24) *National Institute of Advanced Industrial Science and Technology*, SDBS Nr. 4062; http://riodb01.ibase.aist.go.jp/sdbs/ (accessed Jan 31, 2012).
(25) Stuart, B. H. *Infrared Spectroscopy. Fundamentals and Applications*; Wiley: New York, 2004.
(26) Cvitkovic, A.; Ocelic, N.; Hillenbrand, R. Analytical model for quantitative prediction of material contrasts in scattering-type near-field optical microscopy. *Opt. Express* **2007**, *15*, 8550.
(27) Crozier, K. B.; Sundaramurthy, A.; Kino, G. S.; Quate, C. F. Optical antennas: Resonators for local field enhancement. *J. Appl. Phys.* **2003**, *94*, 4632−4642.
(28) Neubrech, F.; et al. Resonant Plasmonic and Vibrational Coupling in a Tailored Nanoantenna for Infrared Detection. *Phys. Rev. Lett.* **2008**, *101*, 157403.
(29) Adato, R.; et al. Ultra-sensitive vibrational spectroscopy of protein monolayers with plasmonic nanoantenna arrays. *Proc. Natl. Acad. Sci.* **2009**, *106*, 19227−19232.
(30) Krutokhvostov, R.; et al. Enhanced resolution in subsurface near-field optical microscopy. *Opt. Express* **2012**, *20*, 593−600.
(31) Magonov, S. N.; Reneker, D. H. Characterization of Polymer Surfaces with Atomic Force Microscopy. *Annu. Rev. Mater. Sci.* **1997**, *27*, 175−222.
(32) Danilov, V.; Wagner, H.-E.; Meichsner, J. Modification of Polydimethylsiloxane Thin Films in H2 Radio-frequency Plasma Investigated by Infrared Reflection Absorption Spectroscopy. *Plasma Processes Polymers* **2011**, *8*, 1059−1067.

■ NOTE ADDED IN PROOF

After acceptance of our manuscript we became aware of a related work demonstrating molecular s-SNOM vibrational spectroscopy by Xu et al. (Xu, X.; Rang, M.; Craig, I.; Raschke, M. Pushing the Sample-Size Limit of Vibrational Nanospectroscopy: From Monolayer toward Single Molecule Sensitivity, *J. Phys. Chem. Lett.* **2012**, 3 (13), 1836-1841).